Cell Biology International ISSN 1065-6995
doi: 10.1002/cbin.10697

RESEARCH ARTICLE

Long non-coding RNA *MIAT* knockdown promotes osteogenic differentiation of human adipose-derived stem cells

Chanyuan Jin[1], Yunfei Zheng[2], Yiping Huang[2], Yunsong Liu[1], Lingfei Jia[3,4]* and Yongsheng Zhou[1,5]*

1 Department of Prosthodontics, Peking University School and Hospital of Stomatology, Beijing 100081, China
2 Department of Orthodontics, Peking University School and Hospital of Stomatology, Beijing 100081, China
3 Department of Oral and Maxillofacial Surgery, Peking University School and Hospital of Stomatology, Beijing 100081, China
4 Central Laboratory, Peking University School and Hospital of Stomatology, Beijing 100081, China
5 National Engineering Laboratory for Digital and Material Technology of Stomatology, Beijing Key Laboratory of Digital Stomatology, Beijing 100081, China

Abstract

Recently, long non-coding RNAs (lncRNAs) have emerged as critical players in gene regulation for multiple biological processes. However, their roles and functions in human adipose-derived stem cells (hASCs) differentiation remain unclear. In the present study, we investigated the role of lncRNA myocardial infarction-associated transcript (*MIAT*) in the osteogenic differentiation of hASCs. We found that the expression of *MIAT* was downregulated in a time-dependent manner during hASCs osteoinduction. *MIAT* knockdown promoted osteogenic differentiation of hASCs both in vitro and in vivo. Moreover, *MIAT* expression was increased upon tumor necrosis factor-α treatment and *MIAT* knockdown reversed the negative effects of inflammation on osteoblastic differentiation. This study improves our knowledge of lncRNAs in governing the osteogenic differentiation of hASCs and may provide novel therapeutic strategies for treating bone diseases.

Keywords: human adipose-derived stem cells; inflammation; lncRNA *MIAT*; osteoblastic

Introduction

Human adipose-derived stem cells (hASCs) are multipotent adult somatic stem cells that can be isolated from adipose tissues (Dai et al., 2016). Their self-renewal ability, high proliferative capacity, and potential for osteogenic differentiation make them a suitable cell type for bone tissue engineering (Rumman et al., 2015). Despite a number of studies on controlling hASCs differentiation into specific lineages by modulating cell signaling pathways, the precise molecular mechanisms of differentiation remain unclear.

Recently, long non-coding RNAs (lncRNAs) have been shown to regulate gene expression at the transcriptional, post-transcriptional, or epigenetic level, and to play important roles in various biological processes and diseases (Lopez-Pajares, 2016; Nie et al., 2016; Schmitz et al., 2016). Several studies have reported that some lncRNAs, such as H19, MEG3, and ANCR, are involved in regulating the osteogenic differentiation of stem cells (Yan et al., 2015; Zhuang et al., 2015; Liang et al., 2016). These findings provide evidence that targeting lncRNAs may provide feasible and effective therapeutics for bone regeneration.

Myocardial infarction-associated transcript (*MIAT*) was one of the lncRNAs first discovered in 2006 (Ishii et al., 2006). It was found to play a critical role in many signaling pathways and to participate in various diseases, such as myocardial infarction, microvascular dysfunction, diabetic retinopathy, and mental disorders (Crea et al., 2016; Shen et al., 2016). However, the role of *MIAT* in osteogenesis is still unknown.

In this study, we first confirmed that *MIAT* affects the osteogenic differentiation of hASCs. In clinical therapeutic bone regeneration, defective or injured tissues are frequently

*Corresponding authors: e-mail: jialingfei1984@sina.com (L.J.); kqzhouysh@hsc.pku.edu.cn (Y.Z.)
Abbreviations: ALP, alkaline phosphatase; ARS, Alizarin red S; BMD, bone mineral density; BV/TV, bone volume/total volume; GAPDH, glyceraldehyde 3-phosphate dehydrogenase; hASCs, human adipose-derived stem cells; lncRNAs, long non-coding RNAs; MIAT, myocardial infarction-associated transcript; OCN, osteocalcin; OM, osteogenic medium; PBS, phosphate-buffered saline; PM, proliferation medium; RUNX2, runt-related transcription factor 2;

in an inflamed condition (Bastian et al., 2011), but inflammation was previously reported to have a negative effect on osteogenesis (Jang et al., 2015; Lin et al., 2016; Wang et al., 2016). Thus, we further investigated whether *MIAT* is involved in the inflammation-related inhibition of osteoblast differentiation. Taken together, these findings are the first to reveal the expression profiles of *MIAT* in the osteogenic differentiation of hASCs, which provides an experimental basis for bone tissue engineering.

Materials and methods

Cell culture and lentiviral transfection

Primary hASCs were obtained from ScienCell Research Laboratories (Carlsbad, CA, USA) and cultured at sub-confluent densities in proliferation medium (PM), made up of Dulbecco's modified Eagle medium supplemented with 10% fetal bovine serum and 1% antibiotics. Cells from three donors were used for the experiments. Osteoblast differentiation of hASCs was induced after they reached 70–80% confluence using standard proliferation medium supplemented with 100 nM dexamethasone, 200 μM L-ascorbic acid, and 10 mM β-glycerophosphate. All cell-based in vitro experiments were repeated in triplicate. Recombinant lentiviruses targeting *MIAT* (sh*MIAT*-1 and sh*MIAT*-2) and the negative control (NC) were obtained from GenePharma Co. (Suzhou, China). Viral packaging and infection were performed as described previously (Zhang et al., 2016). The sequences used for *MIAT* knockdown are shown in Table 1.

Alkaline phosphatase (ALP) staining and activity

ALP staining and activity was performed as described previously (Ge et al., 2011, 2014). Cells were washed three times with phosphate-buffered saline (PBS) and then fixed with 4% paraformaldehyde at room temperature for 10 min. Then, the samples were placed in the dark to undergo ALP staining for 20 min (CWBIO, Beijing, China). Then, they were washed three times with PBS and images were obtained under a scanner. ALP activity was analyzed using an ALP Assay Kit (Nanjing Jian Cheng Bioengineering Institute, Nanjing, China). Total protein content was determined in the same sample by the bicinchoninic acid method using the Pierce Protein Assay Kit (Thermo, Rockford, IL, USA). ALP activity relative to that in the control was calculated after normalization to the total protein content.

Alizarin red S (ARS) staining and quantification

Cells cultured for 14 days in osteogenic medium (OM) were assayed as described previously (Ge et al., 2011, 2014). They were fixed with 4% paraformaldehyde for 10 min at room temperature, washed three more times with double-distilled water, and then stained with 2% ARS staining solution (pH 4.2; Sigma, St. Louis, MO, USA) for 30 min at room temperature. Images were then obtained. For the quantification of mineralization, the stain was solubilized with 100 mM cetylpyridinium chloride (Sigma) for 1 h and then the solution was collected and distributed at 100 μL per well on a 96-well plate for determination of the absorbance at 562 nm using a spectrophotometer (Thermo).

RNA isolation and quantitative reverse transcription polymerase chain reaction (qRT-PCR)

The total RNA was extracted with TRIzol reagent (Invitrogen, Carlsbad, CA, USA) in accordance with the manufacturer's instructions. Then, it was reverse-transcribed in accordance with the manufacturer's instructions (Takara, Tokyo, Japan). Quantitative PCR was performed with SYBR Green Master Mix (Roche Applied Science, Mannheim, Germany) using a 7500 Real-Time PCR Detection System (Applied Biosystems, Foster City, CA, USA) with glyceraldehyde 3-phosphate dehydrogenase (GAPDH) for normalization. The primer sequences are shown in Table 1.

Table 1 Sequences of RNA and DNA Oligonucleotides

Name	Sense strand/sense primer (5′–3′)	Antisense strand/antisense primer (5′–3′)
Primers for qRT-PCR		
MIAT	TCTCTGGTGCTTCCCTCCTT	GATCTAAGCTTGAGCCCCCA
ALP	ATGGGATGGGTGTCTCCACA	CCACGAAGGGGAACTTGTC
RUNX2	CCGCCTCAGTGATTTAGGGC	GGGTCTGTAATCTGACTCTGTCC
OCN	CACTCCTCGCCCTATTGGC	CCCTCCTGCTTGGACACAAAG
GAPDH	GGTCACCAGGGCTGCTTTTA	GGATCTCGCTCCTGGAAGATG
shRNA		
sh*MIAT*-1	GGTCAGGATTAGTGGTCATTC	
sh*MIAT*-2	GGTGATTACCGTGCACCTTGA	
NC	TTCTCCGAACGTGTCACGTTTC	

ALP: alkaline phosphatase; GAPDH: glyceraldehyde 3-phosphate dehydrogenase; OCN: osteocalcin; RUNX2 runt-related transcription factor 2.

Western blot

Western blot was performed as described previously (Jia et al., 2014). Briefly, cells were lysed in radioimmunoprecipitation assay buffer (Sigma) supplemented with protease inhibitor cocktail (Roche). Equal amounts of protein extract were loaded onto gels for 10% sodium dodecyl sulfate polyacrylamide gel electrophoresis. After the electrophoresis, the proteins were transferred to a polyvinylidene fluoride membrane (Millipore, Billerica, MA, USA) and then incubated with primary antibodies against osteocalcin (OCN) (Abcam, Cambridge, UK) and GAPDH (Abcam) at 4°C overnight. The membrane was incubated with goat anti-rabbit IgG (Abcam) and then visualized using ECL Western Blot Kit (CWBIO). Protein level was quantified using the National Institutes of Health ImageJ software (Bethesda, MD, USA). The background was subtracted and the signal of each target band was normalized to that of the GAPDH band.

Heterotopic bone formation assay in vivo

The cells were collected and loaded onto Bio-Oss Collagen (Geistlich, GEWO GmbH, Baden-Baden, Germany) scaffolds and subsequently incubated at 37°C for 3 h, allowing hASCs to attach to the graft. Then, the specimens were followed by centrifugation at 150*g* for 5 min and implanted subcutaneously on the back of 6-week-old BALB/c homozygous nude (nu/nu) mice (10 mice per group). Xenografts were harvested at 8 weeks after implantation and fixed in 4% paraformaldehyde. All animal experiments were approved by Peking University Biomedical Ethics Committee Experimental Animal Ethics Branch.

Micro-computed tomography (CT) analysis

The specimens were harvested at 8 weeks postoperatively and scanned using a high-resolution Inveon Micro-CT (Siemens, Munich, Germany) with an effective pixel size of 9.08 μm, an X-ray source at 80 kV and 500 μA, and an exposure time of 500 ms for each of the 360 rotational steps. Raw images were reconstructed with identical thresholds for all samples using image reconstruction software. Morphometric parameters were determined using the data analysis software Inveon Research Workplace (Siemens, Munich, Germany). The parameters of bone volume/total volume (BV/TV) fraction and bone mineral density (BMD) were compared.

Hematoxylin and eosin (H&E) staining, Masson's trichrome, and immunohistochemistry

Specimens from each group were decalcified in 10% ethylene diamine tetraacetic acid (pH 7.4) for 1 month. Samples were gradually dehydrated and embedded in paraffin. Then, sections (5 μm) were cut and stained with H&E and Masson's trichrome, then subjected to immunohistochemical staining targeting OCN (Abcam) to observe new bone formation under an Olympus microscope (Olympus Co., Tokyo, Japan).

Statistical analysis

The results represent the mean of three independent experiments and data are presented as means ± standard deviations (SDs). Comparisons between groups were analyzed by Student's *t*-tests or analysis of variance for experiments with more than two subgroups. All statistical analyses were performed using GraphPad Prism 5 (GraphPad Software, Inc., La Jolla, CA, USA). A two-tailed *P*-value <0.05 was considered to indicate statistical significance.

Results

MIAT is significantly downregulated in osteogenic differentiation of hASCs

To obtain insight into the involvement of *MIAT* in osteogenic differentiation, we detected its expression profile during this process. Osteogenic differentiation of hASCs was evidenced by the increased expression of genes associated with osteoblast differentiation, namely, *RUNX2*, *ALP*, and *OCN*, at the indicated times (Figures 1A–1C). In contrast, the mRNA expression of *MIAT* was downregulated in a time-dependent manner during the process of hASCs osteogenic differentiation (Figure 1D).

MIAT knockdown significantly promotes the osteogenic differentiation of hASCs in vitro

To further investigate the role of *MIAT* in the osteogenic differentiation of hASCs, we established *MIAT* knockdown hASCs with two different short hairpin RNA sequences. The efficiency of lentiviral transduction was >90% (Figure 1E) and the knockdown efficiency was confirmed by qRT-PCR (Figure 1F).

The ALP activity was significantly increased by *MIAT* knockdown (Figures 2A and 2B). Compared to NC, *MIAT* knockdown significantly increased the mineralization effects in hASCs at day 14 (Figures 2C and 2D). Protein levels of OCN were examined in hASCs cultured with OM for 14 days. *MIAT* knockdown increased the expression of OCN protein, and the fold increases of protein levels were 3.8 and 3.9 compared to those in the NC group (Figures 2E and 2F). We also assessed the mRNA expression of several osteogenic markers after induction. *MIAT* knockdown significantly promoted the mRNA expression of *RUNX2*, *ALP*, and *OCN* (Figures 2G–2I).

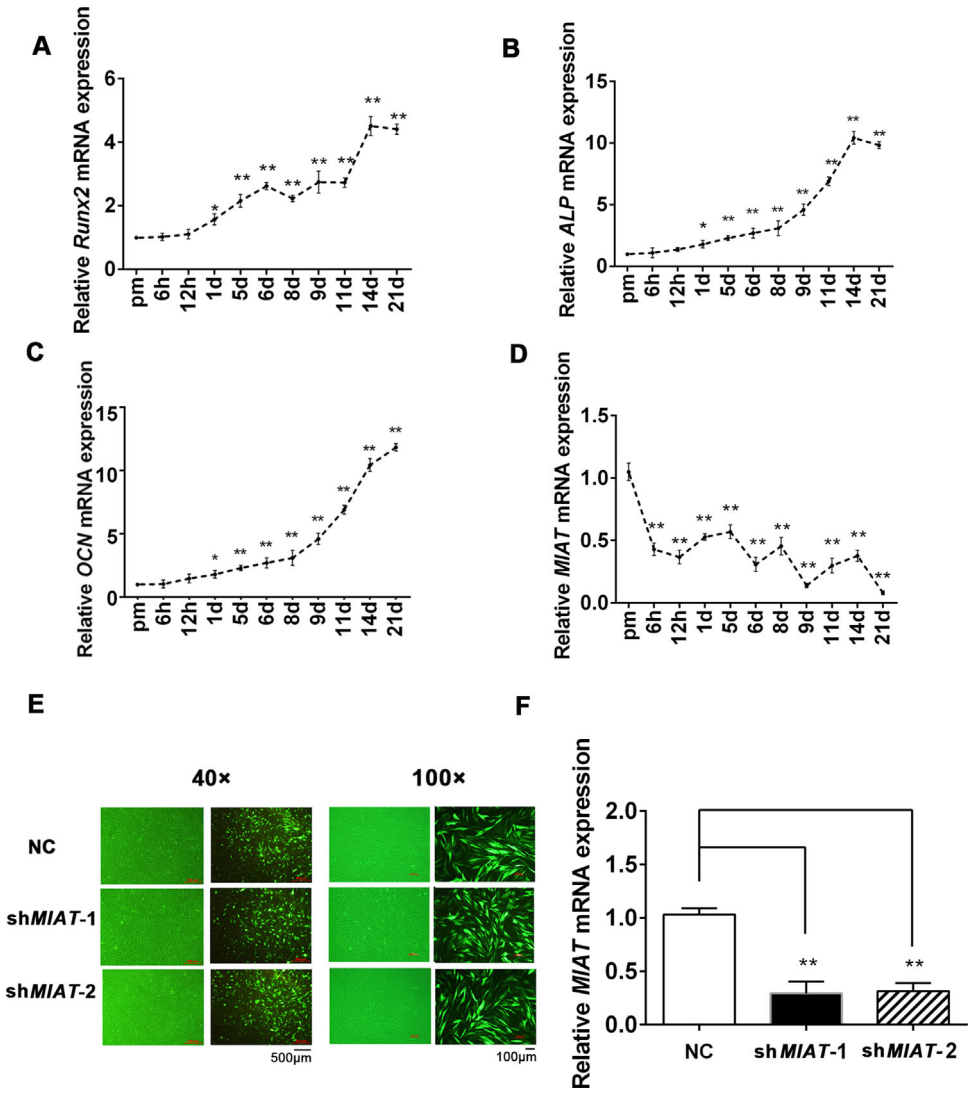

Figure 1 Cells were treated with proliferation medium (PM) or osteogenic induction medium (OM) for 21 days to investigate the change in myocardial infarction-associated transcript (*MIAT*) levels. (A–C) *RUNX2*, alkaline phosphatase (*ALP*), and osteocalcin (*OCN*) expression was increased during the osteogenic differentiation of human adipose-derived stem cells (hASCs). (D) *MIAT* was downregulated in a time-dependent manner during osteogenic differentiation, and glyceraldehyde 3-phosphate dehydrogenase (*GAPDH*) was used as a control. (E) Fluorescent photomicrographs showing the efficiency of lentivirus transduction (>80%) in hASCs sh*MIAT* and negative control (NC). Scale bar = 500 or 100 μm. (F) Knockdown efficiency of *MIAT* in hASCs expressing sh*MIAT*. Results are presented as the mean ± SD (*$P < 0.05$, **$P < 0.01$).

MIAT knockdown accelerates bone formation in vivo

hASCs transfected with sh*MIAT*-1, sh*MIAT*-2, or NC were loaded onto Bio-Oss Collagen scaffolds, and then transplanted subcutaneously into the back of 6-week-old nude mice. After 8 weeks, the transplants were harvested, scanned by micro-CT, and then subjected to histological analysis. Micro-CT showed that BV/TV and BMD were significantly increased in the *MIAT*-knockdown group (Figures 3A and 3B). H&E staining, Masson's trichrome staining, and immunohistochemical staining were consistent with the micro-CT results in showing that new bone formation was greater in the sh*MIAT*-1 and sh*MIAT*-2 groups than in the NC group (Figures 3C).

MIAT knockdown reverses the inhibition of osteogenic differentiation induced by tumor necrosis factor (TNFα)

The expression of *MIAT* was significantly upregulated by TNFα in a time- and dose-dependent manner (Figures 4A and 4B). Because *MIAT* increased during inflammation, we investigated the effects of *MIAT* knockdown on

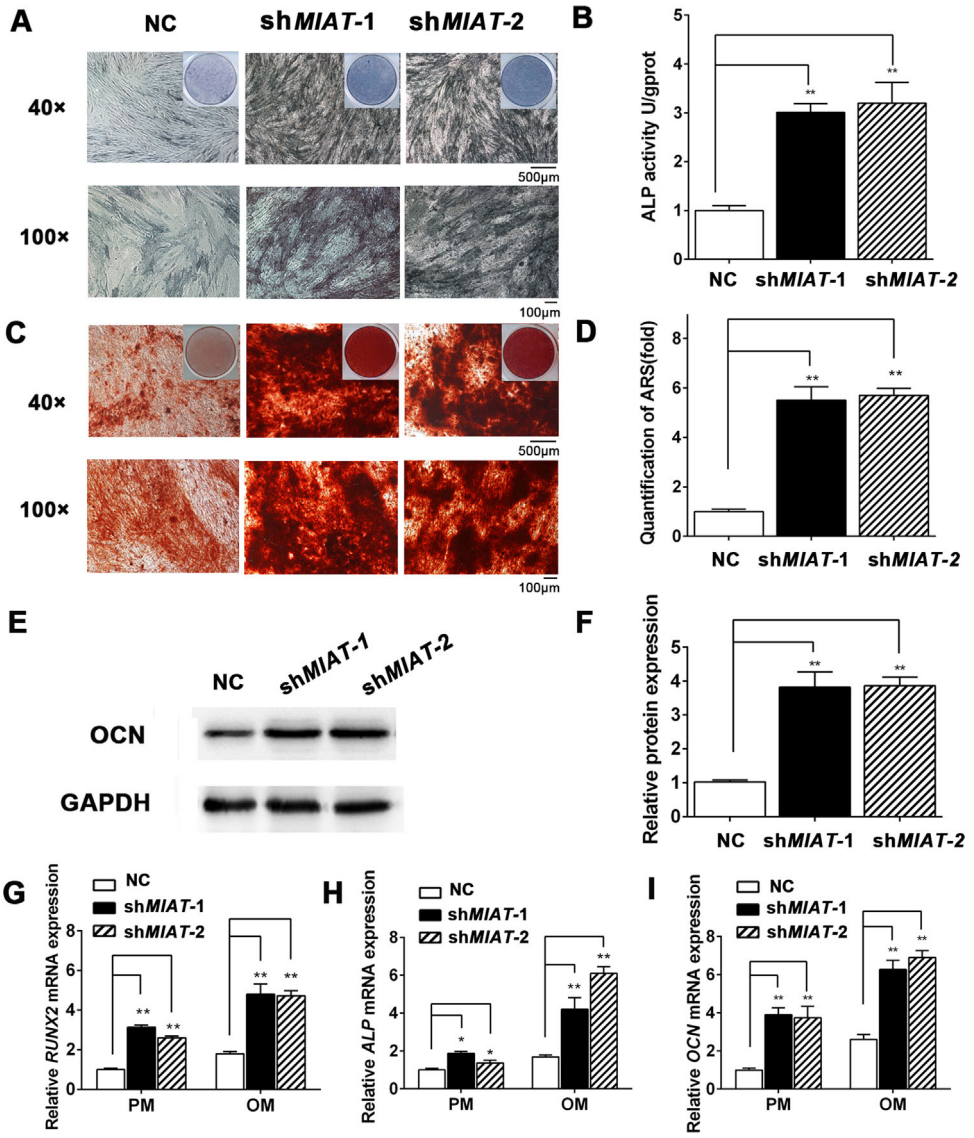

Figure 2 Knockdown of *MIAT* promotes the osteogenic differentiation of hASCs. (A) Images of ALP staining. Scale bars = 500 or 100 μm. (B) ALP activity was determined by ALP assay and is expressed relative to total cellular protein. (C) Alizarin red S (ARS) staining images are from day 14. Scale bars = 500 or 100 μm. (D) Histograms show the quantification of ARS staining by spectrophotometry. (E and F) OCN levels were measured by Western blot, with the internal control GAPDH, at day 14 of osteogenic induction. Histograms show the quantification of band intensities. (G–I) Relative mRNA expression of *RUNX2*, *ALP*, and *OCN* was measured by quantitative reverse transcription polymerase chain reaction (qRT-PCR) at day 14 of osteogenic induction. Results are presented as the mean ± SD ($^{*}P < 0.05$, $^{**}P < 0.01$).

osteogenesis under conditions of inflammation. *MIAT* knockdown dramatically reversed the negative effects of TNFα on osteoblast differentiation, as shown by ALP staining, ALP activity, and mineralized matrix staining (Supplementary Figures S1A–S1D). The reduced protein expression of OCN induced by TNFα treatment was also reversed in *MIAT*-knockdown cells (Supplementary Figures S1E and S1F). The reduced mRNA expression of osteogenesis-related marker genes (*RUNX2*, *ALP*, and *OCN*) induced by TNFα was rescued by *MIAT* knockdown (Supplementary Figures S1G–S1I).

Discussion

The present study confirmed that *MIAT* was downregulated during osteogenic differentiation and *MIAT* knockdown promoted the osteoblastic differentiation of hASCs both in vitro and in vivo.

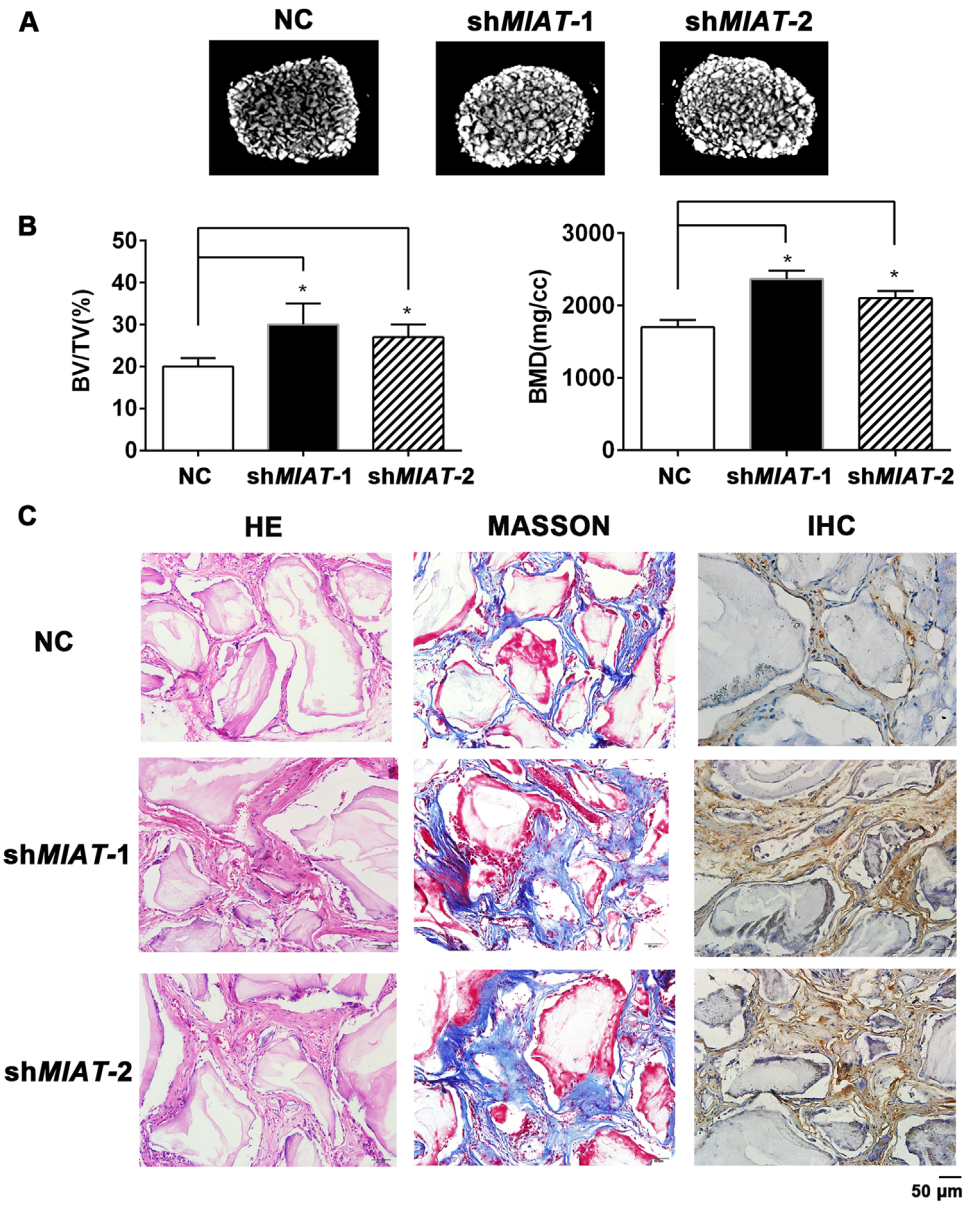

Figure 3 *MIAT* knockdown promoted heterotopic bone formation in vivo. (A) Reconstructed 3D micro-computed tomography images of the tissue-engineered bone constructs from normal control (NC), sh*MIAT*-1, and sh*MIAT*-2 groups. (B) Percentages of new bone volume to tissue volume (BV/TV) and bone mineral density (BMD) of cultured bone constructs. (C) Hematoxylin and eosin staining, Masson's trichrome staining, and immunohistochemical staining of OCN in NC, sh*MIAT*-1, and sh*MIAT*-2 groups. Scale bar: 50 μm. Data are shown as the mean ± SD (*$P < 0.05$).

In recent years, great attention has been paid to deciphering the mechanisms by which lncRNAs regulate the differentiation of stem cells (Qu et al., 2016; Yu and Kuo, 2016). H19 has been reported to play an important role in regulating the osteogenic differentiation of BMSCs. Overexpression of H19 promotes the osteogenic differentiation of BMSCs, whereas knockdown of H19 inhibits these effects (Huang et al., 2015). lncRNA AK141205 has also been shown to play important roles in regulating the osteogenic growth peptide-induced formation of calcium salt nodules, ALP activity, and osteogenic differentiation-associated gene expression (Calin and Croce, 2006). Moreover, downregulated ANCR promotes the proliferation and osteogenic differentiation of periodontal ligament stem cells by upregulating the expression of osteogenic differentiation marker genes (Yan et al., 2015).

MIAT has been reported to be involved in various diseases, and pathological and physiological processes such

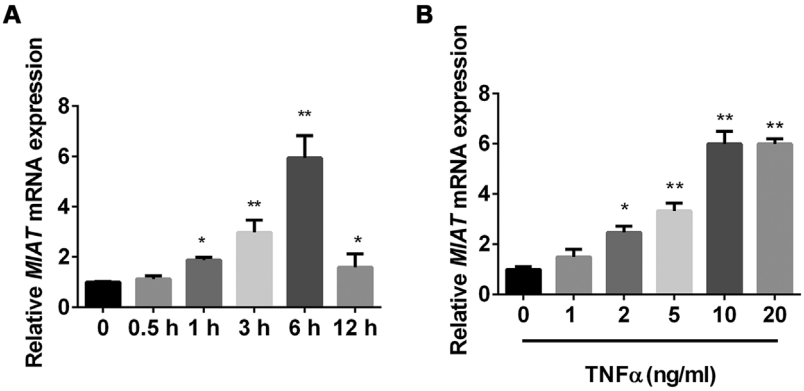

Figure 4 The expression of *MIAT* was significantly upregulated by TNFα in a time- and dose-dependent manner. (A) Relative expression of *MIAT* in hASCs stimulated with TNFα for the time indicated by qRT-PCR, normalized by *GAPDH*, relative to untreated groups. (B) Relative expression of *MIAT* in hASCs stimulated with TNFα for the indicated concentrations. (*$P < 0.05$, **$P < 0.01$).

as myocardial infarction, diabetic retinopathy, paranoid schizophrenia, microvascular dysfunction, the formation of nuclear bodies, and neurogenic commitment (Yan et al., 2015; Zhou et al., 2015; Liao et al., 2016). However, the precise roles of *MIAT* in regulating osteogenic differentiation remain unexplored. This study confirmed the previously uncharacterized roles of *MIAT* in regulating the osteogenic differentiation of hASCs.

Furthermore, we discovered that *MIAT* can be upregulated by TNFα, and knockdown of *MIAT* can rescue the inhibition of osteogenesis induced by inflammation. It has been reported that inflammation is a potential risk factor for osteoporosis because proinflammatory cytokines, such as interleukin-1 (IL-1), IL-6, and TNFα, are crucial mediators of bone resorption (Hofbauer et al., 2000). Proinflammatory cytokines, such as TNFα, have been reported to inhibit the differentiation of osteoblasts from precursor cells in vitro as well as fracture repair in vivo (Gilbert et al., 2000; Neumann et al., 2014). Hence, it is necessary to develop more effective therapies targeting TNFα to alleviate chronic inflammation-related bone diseases. The present study was consistent with previous studies in showing that the osteogenic differentiation of hASCs was inhibited by TNFα at a concentration of 10 ng/mL (Chang et al., 2013). Subsequent experiments showed that *MIAT* was significantly upregulated and displayed an oscillation pattern consistent with TNFα stimulation patterns. We detected the effects of *MIAT* knockdown on the TNFα-induced inhibition of osteogenesis. The results showed that *MIAT* knockdown could rescue the TNFα-induced inhibition of the osteogenic differentiation of hASCs.

MIAT plays important roles in inflammation-related processes; for example, it alleviates retinal inflammation under diabetic conditions (Yan et al., 2015). Interestingly, it also acts as a miR-150-5p sponge and regulates its binding to target mRNAs. It may also function as a competing endogenous RNA by forming a feedback loop with Akt and miR-150-5p to regulate human lens epithelial cell function upon oxidative stress and inflammatory factor stimulus (Shen et al., 2016). Thus, it is not surprising that *MIAT* knockdown can reverse the inflammation-induced inhibition of osteogenesis. However, the precise role and underlying mechanism have remained unexplored. Further detailed research needs to be performed to confirm the molecular signals involved.

Taken together, our results suggest that the knockdown of *MIAT* not only promotes osteogenic differentiation but also reverses the inhibitory effects of TNFα on osteogenesis. Our data may lead to many therapeutic applications for tissue engineering and regenerative medicine.

Conclusions

In conclusion, our data indicate that *MIAT* acts as an important regulator of osteogenic differentiation of hASCs. *MIAT* knockdown not only promotes osteogenic differentiation but also reverses the inhibitory effects of TNFα on osteogenesis.

Acknowledgments and funding

Chanyuan Jin: performed the experiments and wrote the paper; Yunfei Zheng, Yiping Huang, and Yunsong Liu: collection and/or assembly of data; Yongsheng Zhou and Lingfei Jia: conception and design, financial support, manuscript writing, and final approval of manuscript. This study was financially supported by grants from the National Natural Science Foundation of China (No. 81371118, No. 81402235), the Program for New Century Excellent Talents in University from Ministry of Education of China (NCET-11-0026), the Ph.D. Programs Foundation of Ministry of Education of China (No. 20130001110101),

and grants from the PKU School of Stomatology for Talented Young Investigators (PKUSS20140104).

Conflict of interest

The authors have no conflict of interest to disclose.

References

Bastian O, Pillay J, Alblas J, Leenen L, Koenderman L, Blokhuis T (2011) Systemic inflammation and fracture healing. J Leukoc Biol 89(5): 669–73.

Calin GA, Croce CM (2006) MicroRNA signatures in human cancers. Nat Rev Cancer 6(11): 857–66.

Chang J, Liu F, Lee M, Wu B, Ting K, Zara JN, Soo C, Al Hezaimi K, Zou W, Chen X, Mooney DJ, Wang CY (2013) NF-kappaB inhibits osteogenic differentiation of mesenchymal stem cells by promoting beta-catenin degradation. Proc Natl Acad Sci USA 110(23): 9469–74.

Crea F, Venalainen E, Ci X, Cheng H, Pikor L, Parolia A, Xue H, Nur Saidy NR, Lin D, Lam W, Collins C, Wang Y (2016) The role of epigenetics and long noncoding RNA MIAT in neuroendocrine prostate cancer. Epigenomics 8(5): 721–31.

Dai R, Wang Z, Samanipour R, Koo KI, Kim K (2016) Adipose-derived stem cells for tissue engineering and regenerative medicine applications. Stem Cells Int 2016: 6737345.

Ge W, Liu Y, Chen T, Zhang X, Lv L, Jin C, Jiang Y, Shi L, Zhou Y (2014) The epigenetic promotion of osteogenic differentiation of human adipose-derived stem cells by the genetic and chemical blockade of histone demethylase LSD1. Biomaterials 35(23): 6015–25.

Ge W, Shi L, Zhou Y, Liu Y, Ma GE, Jiang Y, Xu Y, Zhang X, Feng H (2011) Inhibition of osteogenic differentiation of human adipose-derived stromal cells by retinoblastoma binding protein 2 repression of RUNX2-activated transcription. Stem Cells 29(7): 1112–25.

Gilbert L, He X, Farmer P, Farmer P, Boden S, Kozlowski M, Rubin J, Nanes MS (2000) Inhibition of osteoblast differentiation by tumor necrosis factor-alpha. Endocrinology 141(11): 3956–64.

Hofbauer LC, Khosla S, Dunstan CR, Lacey DL, Boyle WJ, Riggs BL (2000) The roles of osteoprotegerin and osteoprotegerin ligand in the paracrine regulation of bone resorption. J Bone Miner Res 15(1): 2–12.

Huang Y, Zheng Y, Jia L, Li W (2015) Long noncoding RNA H19 promotes osteoblast differentiation via TGF-beta1/Smad3/HDAC signaling pathway by deriving miR-675. Stem Cells 33(12): 3481–92.

Ishii N, Ozaki K, Sato H, Mizuno H, Saito S, Takahashi A, Miyamoto Y, Ikegawa S, Kamatani N, Hori M, Saito S, Nakamura Y, Tanaka T (2006) Identification of a novel non-coding RNA, MIAT, that confers risk of myocardial infarction. J Hum Genet 51(12): 1087–99.

Jang WG, Jeong BC, Kim EJ, Choi H, Oh SH, Kim DK, Koo SH, Choi HS, Koh JT (2015) Cyclic AMP response element-binding protein H (CREBH) mediates the inhibitory actions of tumor necrosis factor alpha in osteoblast differentiation by stimulating smad1 degradation. J Biol Chem 290(21): 13556–66.

Jia LF, Wei SB, Gan YH, Guo Y, Gong K, Mitchelson K, Cheng J, Yu GY (2014) Expression, regulation and roles of miR-26a and MEG3 in tongue squamous cell carcinoma. Int J Cancer 135(10): 2282–93.

Liang WC, Fu WM, Wang YB, Sun YX, Xu LL, Wong CW, Chan KM, Li G, Waye MM, Zhang JF (2016) H19 activates Wnt signaling and promotes osteoblast differentiation by functioning as a competing endogenous RNA. Sci Rep 6: 20121.

Liao J, He Q, Li M, Chen Y, Liu Y, Wang J (2016) LncRNA MIAT: myocardial infarction associated and more. Gene 578(2): 158–61.

Lin TH, Gibon E, Loi F, Pajarinen J, Cordova LA, Nabeshima A, Lu L, Yao Z, Goodman SB (2016) Decreased osteogenesis in mesenchymal stem cells derived from the aged mouse is associated with enhanced NF-kappaB activity. J Orthop Res doi: 10.1002/jor.23270

Lopez-Pajares V (2016) Long non-coding RNA regulation of gene expression during differentiation. Pflugers Arch 468(6): 971–81.

Neumann E, Muller-Ladner U, Frommer KW (2014) Inflammation and bone metabolism. Z Rheumatol 73(4): 342–8.

Nie S, Xu J, Zhang C, Xu C, Liu M, Yu D (2016) Salicortin inhibits osteoclast differentiation and bone resorption by down-regulating JNK and NF-kappaB/NFATc1 signaling pathways. Biochem Biophys Res Commun 470(1): 61–7.

Qu Q, Fang F, Wu B, Hu Y, Chen M, Deng Z, Ma D, Chen T, Hao Y, Ge Y (2016) The Potential role of long noncoding RNA in the osteogenic differentiation of human periodontal ligament stem cells. J Periodontol 87(7): e127–37.

Rumman M, Dhawan J, Kassem M (2015) Concise review: quiescence in adult stem cells: biological significance and relevance to tissue regeneration. Stem Cells 33(10): 2903–12.

Schmitz SU, Grote P, Herrmann BG (2016) Mechanisms of long noncoding RNA function in development and disease. Cell Mol Life Sci 73(13): 2491–509.

Shen Y, Dong LF, Zhou RM, Yao J, Song YC, Yang H, Jiang Q, Yan B (2016) Role of long non-coding RNA MIAT in proliferation, apoptosis and migration of lens epithelial cells: a clinical and in vitro study. J Cell Mol Med 20(3): 537–48.

Wang N, Zhou Z, Wu T, Liu W, Yin P, Pan C, Yu X (2016) TNF-alpha-induced NF-kappaB activation upregulates microRNA-150-3p and inhibits osteogenesis of mesenchymal stem cells by targeting beta-catenin. Open Biol 6(3): pii: 150258.

Yan B, Yao J, Liu JY, Li XM, Wang XQ, Li YJ, Tao ZF, Song YC, Chen Q, Jiang Q (2015) LncRNA-MIAT regulates microvascular dysfunction by functioning as a competing endogenous RNA. Circ Res 116(7): 1143–56.

Yu CY, Kuo HC (2016) The trans-spliced long noncoding RNA tsRMST impedes human ESC differentiation through WNT5A-mediated inhibition of the epithelial-to-mesenchymal transition. Stem Cells 34(8): 2052–62.

Zhang P, Liu Y, Jin C, Zhang M, Tang F, Zhou Y (2016) Histone acetyltransferase GCN5 regulates osteogenic differentiation of mesenchymal stem cells by inhibiting NF-kappaB. J Bone Miner Res 31(2): 391–402.

Zhou L, Xu DY, Sha WG, Shen L, Lu GY, Yin X (2015) Long non-coding MIAT mediates high glucose-induced renal tubular epithelial injury. Biochem Biophys Res Commun 468(4): 726–32.

Zhuang W, Ge X, Yang S, Huang M, Zhuang W, Chen P, Zhang X, Fu J, Qu J, Li B (2015) Upregulation of lncRNA MEG3 promotes osteogenic differentiation of mesenchymal stem cells from multiple myeloma patients by targeting BMP4 transcription. Stem Cells 33(6): 1985–97.

Received 20 June 2016; accepted 25 October 2016.
Final version published online 16 November 2016.

Supporting Information

Additional supporting information may be found in the online version of this article at the publisher's web-site.

Figure S1. *MIAT* knockdown reversed the inhibition of osteogenic differentiation induced by TNFα. hASCs were transfected with scramble shRNA (NC) or two shRNAs (sh*MIAT*-1, sh*MIAT*-2) targeting *MIAT*, then treated with PBS (as control) or TNFα (10 ng/mL) during osteogenic differentiation. (A) ALP staining were performed in NC (with PBS), NC+TNFα, sh*MIAT*-1+TNFα, and sh*MIAT*-2 +TNFα at day 7. Scale bars = 500 or 100 μm. (B) Histogram shows ALP activity. (C) ARS staining images are from day 14. Scale bars = 500 or 100 μm. (D) Quantification of ARS staining by spectrophotometry. (E) Western blot of protein expression of OCN and the internal control GAPDH at day 14 of osteogenic induction. (F) Histograms show the quantification of band intensities. (G–I) Relative mRNA expressions of *RUNX2*, *ALP*, and *OCN* were measured by qRT-PCR at day 14 of osteogenic induction. *GAPDH* was used for normalization. Data are presented as the mean ± SD ($^{**}P < 0.01$).